Styrene–Butadiene Rubber/Graphite Powder Composites: Rheometrical, Physicomechanical, and Morphological Properties

M. N. Ismail, A. I. Khalaf

Polymers and Pigments Department, National Research Center, Dokki, Cairo, Egypt

Received 24 November 2009; accepted 26 July 2010
DOI 10.1002/app.33101
Published online 13 October 2010 in Wiley Online Library (wileyonlinelibrary.com).

ABSTRACT: The physicomechanical properties, curing characteristics, and morphological behaviors of styrene–butadiene rubber/graphite powder composites were evaluated. Different weight fractions and particle sizes of graphite powder were used. An increase in the graphite content increased the maximum torque, reinforcing factor, and tensile strength and decreased the elongation at break and equilibrium swelling. Also, a decrease in the particle size of the graphite increased the tensile strength and decreased the equilibrium swelling. Moreover, the dielectric properties were measured at about 30°C and 100 Hz. The values of permittivity and dielectric loss were found to increase with increasing graphite content. © 2010 Wiley Periodicals, Inc. J Appl Polym Sci 120: 298–304, 2011

Key words: composites; curing of polymers; dielectric properties; mechanical properties; swelling

INTRODUCTION

Elastomers are important polymeric materials because of their unique elastic properties. However, the reinforcement of these elastomers is essential for the realization of the required properties for many different practical applications. Rubber is an elastomer, and the characteristic of rubber elasticity for practical application is provided by vulcanization and the formation of compounds with fillers.[1,2] A vast number of products with specific properties of elasticity, stretching, tear resistance, and abrasion resistance can be made of rubber. These properties can be achieved by the addition of various types of fillers and/or reinforcing additives. Gum natural rubber vulcanizates, although they have high physical strength, are suitable for only very few commercial applications. Fillers are extensively used in the rubber industry, not only to reinforce the polymer matrix but also to improve the rubber processing and, in some cases, to reduce the price of the final material.[3,4] In the case of amorphous polymer-like styrene–butadiene rubber (SBR), which does not undergo strain-induced crystallization, the use of fillers can improve the processability and mechanical properties and reduce the cost of rubber articles.[5,6] In rubber reinforcement, the most important characteristic of the reinforcing filler is that its size must be small, so that the filler particles have a large surface area to interact with rubber.[7,8] In addition to the particle size, the particle structure and surface chemistry are also influential factors in determining the filler's reinforcing efficiency. Fillers are usually made up of primary particles at the smallest size scale; these are strongly bound to other primary particles to form an aggregated structure. These aggregates can interact with other aggregates through weaker secondary bonds to form agglomerates. The interactions between fillers and rubber have a significant effect on the reinforcing properties of a filled rubber, particularly on the filler–filler and filler–rubber interactions.[9–11] Carbon black is the most widely used filler in rubber technology.[12] In addition to reinforcing effects caused by the fractal nature of both carbon black aggregates and larger scale filler networks in the rubber matrix, the surface activity plays a key role in controlling the polymer–filler interactions and, therefore, the overall reinforcement.[13–16]

The effects of reinforcing carbon black on the network structure, technical properties, failure mode, and dielectric properties of natural rubber have been reported.[17–20] Studies on the physicomechanical and/or dielectric properties of SBR were reported in refs. 21–27.

Graphite is a widely used solid lubricant.[28] Graphite is naturally abundant and used as a conducting filler in the preparation of conducting polymer composites. Graphite-filled rubber materials have a small compression set.[29]

Correspondence to: A. I. Khalaf (aman2502003@yahoo.com).

TABLE I
SBR/Graphite Composite Formulations with Different Concentrations of Graphite with Various Particle Sizes (<53, 53–90, 90–125, and 125–150 μm)

SBR (phr)	100	100	100	100	100	100	100	100
ZnO (phr)	2.5	2.5	2.5	2.5	2.5	2.5	2.5	2.5
Stearic acid (phr)	1.5	1.5	1.5			1.5	1.5	1.5
Graphite powder (phr)	0	10	30	50	70	90	110	140
Processing oil (phr)	3	3	3	3	3	3	3	3
CBS (phr)	1.25	1.25	1.25	1.25	1.25	1.25	1.25	1.25
Sulfur (phr)	2.5	2.5	2.5	2.5	2.5	2.5	2.5	2.5

The aim of this study was to study the effect of different concentrations and different particle sizes of graphite filler on the physicomechanical and rheometrical properties of general purpose rubbers such as SBR.

EXPERIMENTAL

Materials

SBR 1502, with a specific gravity of 0.945, supplied by ESSO Chemie (Hamburg, Germany) was used. 2-Graphite was used as a filler with different particle sizes (<53, 53–90, 90–125, and 125–150 μm). The curing system selected contained various compounds, such as *N*-cyclohexyl benzothiazyle sulfonamide (CBS) and sulfur. The activators were zinc oxide (ZnO) and stearic acid. The plasticizer used was naphthenic processing oil (specific gravity = 0.94–0.96). All of the rubber ingredients were supplied by Aldrich Co. (Munich, Germany) and are listed in Table I.

Preparation of the rubber compounds

Rubber was premixed with all of the compounding ingredients according to ASTM D 3182-07. Mixing was done on a laboratory two-roll mill (Florida, USA). The speed of the slow roll was 24 rev/min, with a gear ratio of 1 : 1.4. The compounded rubbers were left overnight before vulcanization. The vulcanization was carried out at 152 ± 1°C for the predetermined

TABLE II
Curing Properties of SBR/Graphite Composites with Different Concentrations of Graphite with Various Particle Sizes (<53, 53–90, 90 –125, and 125–150 μm) at 152 ± 1°C

	Graphite loading (phr)							
Curing property	0	10	30	50	70	90	110	140
<53 μm								
M_L (dN m)	8	8	8	8	10	12	12	12
M_H (dN m)	63	82	90	96	107	116	126	136
$M_H - M_L$ (dN m)	55	74	82	88	97	104	114	124
t_{c90} (min)	27	24	20	18	16	15	16	16
t_{s2} (min)	14.5	13.5	10.5	11	10	9.5	9	7.5
CRI (min^{-1})	8	9.5	10.5	14.3	16.7	18.2	14.3	11.8
53–90 μm								
M_L (dN m)	8	6.5	7.75	8	12	11	13	13
M_H (dN m)	63	76	87.5	95	104	113	122	134
$M_H - M_L$ (dN m)	55	69.5	79.75	87	92	102	109	121
t_{c90} (min)	27	25	22	22	23	19	19	17
t_{s2} (min)	14.5	14	11.5	11	11.5	9.5	9.1	8
CRI (min^{-1})	8	7.17	9.5	9.1	8.7	10.5	10	11.1
90–125 μm								
M_L (dN m)	8	8	10	10	10	11	14	14
M_H (dN m)	63	73	8	9	99	111	116	127
$M_H - M_L$ (dN m)	55	65	70	83	89	100	102	113
t_{c90} (min)	27	24	19	17.5	18	17	16	17
t_{s2} (min)	14.5	13	10.5	9.5	9	9	8.5	8.5
CRI (min^{-1})	8	9.1	11.8	12.5	11.1	12.5	13.3	11.8
125–150 μ								
M_L (dN m)	8	8	8	10	10	12	12	14
M_H (dN m)	63	66	76	87	90	102	106	116
$M_H - M_L$ (dN m)	55	58	68	77	80	90	94	102
t_{c90} (min)	27	23	22.5	21.5	18.5	18	18	16
t_{s2} (min)	14.5	15.5	14	12.5	11.5	11	10	8
CRI (min^{-1})	8	13.3	11.8	11.1	14.3	14.3	12.5	12.5

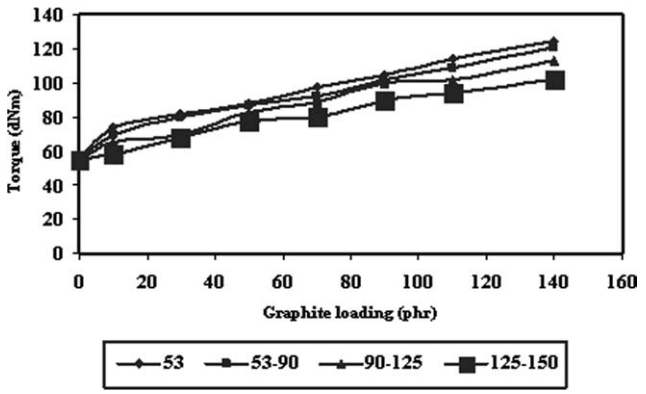

Figure 1 Rheographs of SBR vulcanizates filled with graphites of different particle sizes (53–150 μm).

optimum cure time (t_{c90}) samples in an electrically heated press under a pressure of about 4 MPa to get vulcanized rubber sheets 2 mm thick.

Techniques

Determination of the cure characteristics

Minimum torque (M_L), maximum torque (M_H), t_{c90}, scorch time (t_{s2}), and curing rate index (CRI) were determined according to ASTM D 2084-07 with a Monsanto oscillating disc rheometer (model 100, Akron, OH). The measurements were carried out at 152 ± 1°C.

Mechanical properties

The tensile strength and elongation at break measurements were carried out at room temperature on a tensile testing machine (Zwick 1425, Ulm) according to ASTM D 412-06.

Swelling study

We carried out the swelling tests by putting the samples in toluene at room temperature for 24 h.

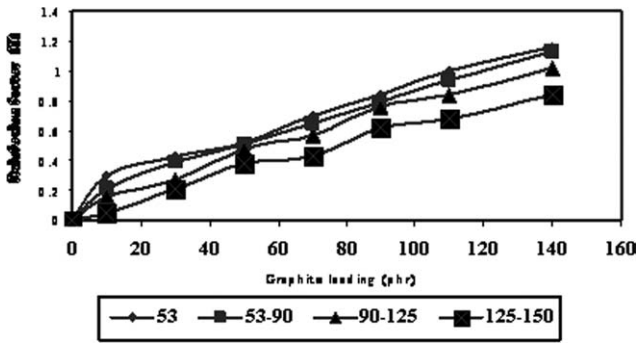

Figure 2 α_f versus the graphite loading with different particle sizes (53–150 μm).

The equilibrium swelling in toluene (Q; %) was measured according to the standard method (ASTM D 471-06). Q was calculated according to

$$Q\% = [(w_s - w_d)/w_d] \times 100$$

where w_s is the weight of the swelled specimen and w_d is the weight of the dried specimen.

Scanning electron microscopy (SEM)

A scanning electron microscope (JEOL JSM-T20, Tokyo, Japan) was used. Nonconductive samples, which include most polymers, are coated with evaporated heavy metal to make an electrical connection between the sample and the specimen stage. Our samples were coated with gold film.

Dielectric measurements

Measurements of the permittivity (ε′) and dielectric loss (ε″) for the various vulcanizates were carried out at fixed frequency (100 Hz) and at room temperature (~ 30°C) with an Inductance, Resistance,

TABLE III
Mechanical Properties of SBR/Graphite Composites with Different Concentrations of Graphite with Various Particle Sizes (<53, 53–90, 90 –125, and 125–150 μm)

	Graphite loading (phr)							
Mechanical property	0	10	30	50	70	90	110	140
<53 μm								
Tensile strength (MPa)	1.03	1.35	2.15	2.55	2.9	3.45	4	4.35
Elongation at break (%)	235	225	205	177	155	130	104	80
53–90 μm								
Tensile strength (MPa)	1.03	1.27	1.95	2.37	2.68	3.17	3.86	121
Elongation at break (%)	235	206	176	158	140	120	95	74
90–125 μm								
Tensile strength (MPa)	1.03	1.19	1.77	2.13	2.35	2.8	3.6	3.85
Elongation at break (%)	235	205	160	149	130	110	83	70
125–150 μm								
Tensile strength (MPa)	1.03	1.15	1.57	1.92	2.14	2.3	2.8	3.25
Elongation at break (%)	235	187	154	142	120	100	80	67

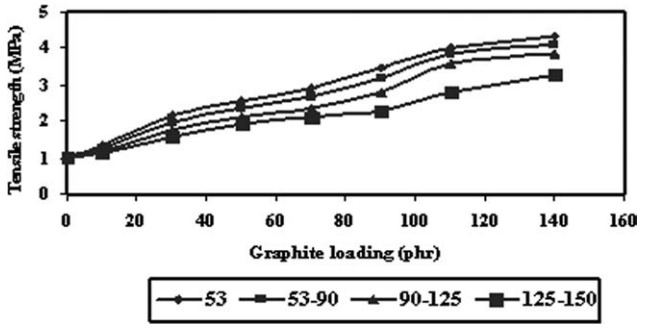

Figure 3 Variation of the tensile strength of the SBR vulcanizates with the graphite loading with different particle sizes (53–150 μm).

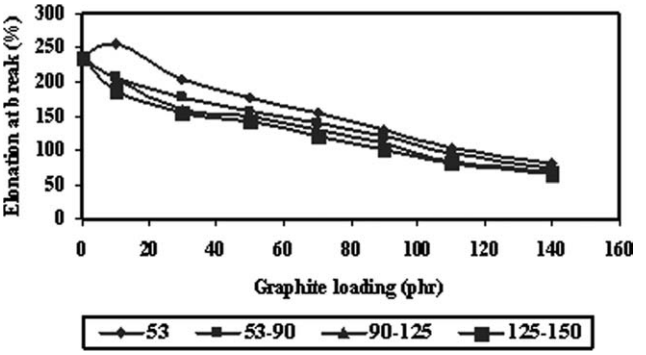

Figure 4 Variation of the elongation at break of the SBR vulcanizates with the graphite loading with different particle sizes (53–150 μm).

Capacitance (LRC) meter (digital bridge type AG-4311B, from ANDO Electric Co., Ltd., Tokyo, Japan).

For dielectric measurements, a guard-ring capacitor (type NFM 5/T, WTW, Ulm, Germany) was used. The thickness and capacitance of the sample were measured in a single compression. The cell temperature were controlled with an ultrathermostat.

The cell was calibrated with plates of known ε' values, such as air, trolitul, and glass with different thicknesses ranging from 2 to 7 mm. The errors in ε' and ε'' amounted to ± 2 and $\pm 5\%$, respectively. The samples were prepared in the form of discs 50 mm in diameter and 3 mm thick.

RESULTS AND DISCUSSION

Curing characteristics

M_H, M_L, and the difference between M_H and M_L increased with the addition of graphite powder (Table II). The difference between M_H and M_L is a rough measure of the crosslink density in the samples and is usually known as the *state of cure*.[30] The state of cure increased with the loading of the graphite in all cases (Fig. 1). This was an indication of the improvement in the graphite filler–SBR matrix adhesion. CRI was proportional to the average slope of the curing curve $[100/(t_{c90} - t_{s2})]$ in the step region. The higher the value of CRI was, the faster the curing process was. t_{s2} increased, t_{c90} decreased, and CRI increased with the addition of graphite. Also, the state of cure depended on the particle size (Fig. 1). As the particle size increased, the state of cure decreased; t_{s2}, t_{c90}, and CRI did not change very much with particle size.

The changes in the rheometric torque with filler loading were used to characterize the filler–matrix interaction or reinforcement, that is, the reinforcing factor (α_f), which was calculated from the rheographs:[31]

$$\alpha_f = \Delta L_{\max}(\text{filled}) - \Delta L_{\max}(\text{gum})/\Delta L_{\max}(\text{gum})$$

where $\Delta L_{\max}$(filled) and $\Delta L_{\max}$(gum) are the changes in torque during vulcanization for the filled and gum compounds, respectively. The plots are given in Figure 2; clearly, as shown in Figure 2, the α_f values increased with increasing graphite content. Also, α_f increased with smaller particle sizes; this indicated a large reinforcement. t_{c90} of the samples filled with graphite was lower than that of the unfilled sample and also decreased with increasing graphite concentration. That is, graphite accelerated the reaction between the sulfur and rubber compounds.[32]

Mechanical properties

The mechanical properties of graphite-powder-filled SBR are summarized in Table III and are illustrated in Figures 3 and 4. Figure 3 shows a remarkable

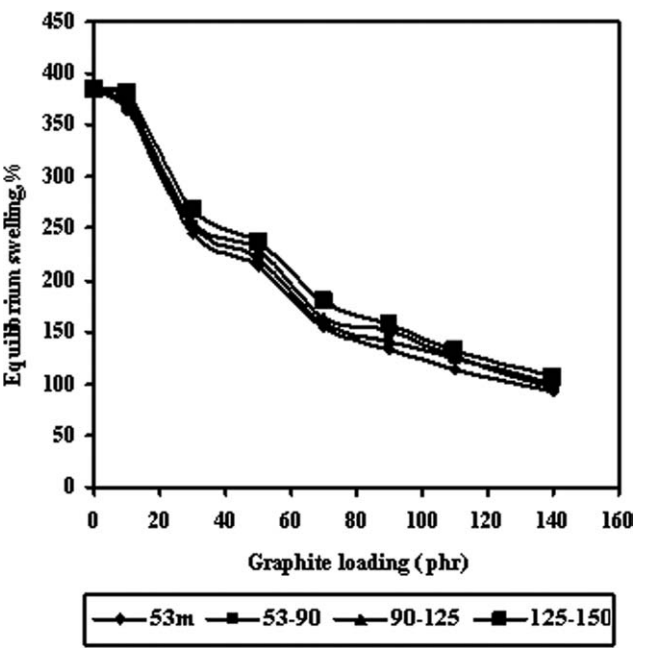

Figure 5 Variation of Q of the SBR vulcanizates with the graphite loading with different particle sizes (53–150 μm).

TABLE IV
Swelling Properties and ν Values of SBR/Graphite Composites with Different Concentrations of Graphite with Various Particle Sizes (<53, 53–90, 90 –125, and 125–150 μm)

Swelling property	Graphite loading (phr)							
	0	10	30	50	70	90	110	140
<53 μm								
Q_m, maximum equilibrium swelling	3.85	3.65	2.89	2.14	1.54	1.33	1.14	0.93
$\nu \times 10^5$ (mol/cm^3)	5.95	6.62	14.5	18.9	35.3	46.1	60.5	85.4
M_c (g/mol)	8397	7548	3454	2635	1416	1085	826	585
53–90 μm								
Q_m	3.85	3.7	2.52	2.21	1.54	1.59	1.24	0.96
$\nu \times 10^5$ (mol/cm^3)	5.95	6.45	13.8	17.8	33.2	42.0	52.2	81.1
M_c (g/mol)	8397	7756	3621	2804	2804	1189	967	617
90–125 μm								
Q_m	3.85	3.76	2.57	2.3	1.64	1.51	1.27	1
$\nu \times 10^5$ (mol/cm^3)	5.95	6.24	13.3	16.5	31.4	36.6	50.1	75.7
M_c (g/mol)	8397	8009	3763	3029	1590	1365	999	660
125–150 μm								
Q_m	3.85	3.8	2.68	2.37	1.84	1.56	1.32	1.07
$\nu \times 10^5$ (mol/cm^3)	5.95	6.11	12.2	15.6	26.4	34.5	46.4	67.5
M_c (g/mol)	8397	8181	4086	3212	1894	1450	1070	741

increase in the tensile strength with increasing graphite content. This shows that graphite acted as a reinforcing filler in the SBR matrix. On the other hand, the elongation at break decreased with increasing graphite loading (Fig. 4). As also shown in these two figures, as the particle size of the graphite increased, the tensile strength and elongation at break of the SBR/graphite composites decreased. This increase in elongation at break was attributed to the sliding effect of fine graphite particles, which could be taken as a plasticization effect.

Q and crosslinking density (ν)

Figure 5 shows the swelling resistance of the rubber vulcanizates filled with graphite powder at different concentrations and different particle sizes. The values obtained for the SBR vulcanizates filled with graphite were lower than that of the gum SBR compound. This indicated that the graphite-filled SBR vulcanizates had more resistance than the unfilled SBR vulcanizate. As the concentration of graphite increased, the swelling decreased because of the good dispersion of graphite and strong interactions between the graphite and polymer matrix.

We also noticed that the swelling index values increased with increasing of particle size, while they decreased with increasing of graphite content. This observation indicated an increase in ν for the filled compounds and that graphite was a good reinforcement in the SBR vulcanizates.

ν ($\nu = 1/2M_c$) was determined with the following Flory–Rehner relation:[23,33]

$$M_c = -\rho V_s V_r^{1/3}/[\ln(1 - V_r) + V_r + \chi V_r^2]$$

where M_c, is the molecular weight between two successive crosslinks, ρ is the density of SBR ($\rho = 0.94$ g/cm^3), V_s is the molar volume of the solvent (toluene; $V_s = 106.35$ cm^3/mol), V_r is the volume fraction of the swollen rubber, which can be obtained from the mass and densities of the rubber samples and

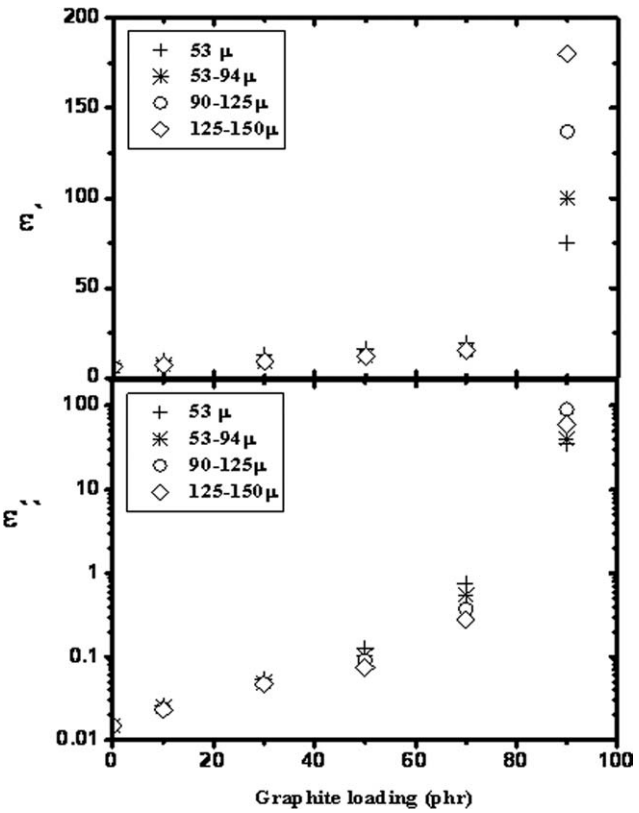

Figure 6 Variation of ε′ and ε″ of the SBR vulcanizates with the graphite loading with different particle sizes (53–150 μm) at 100 Hz.

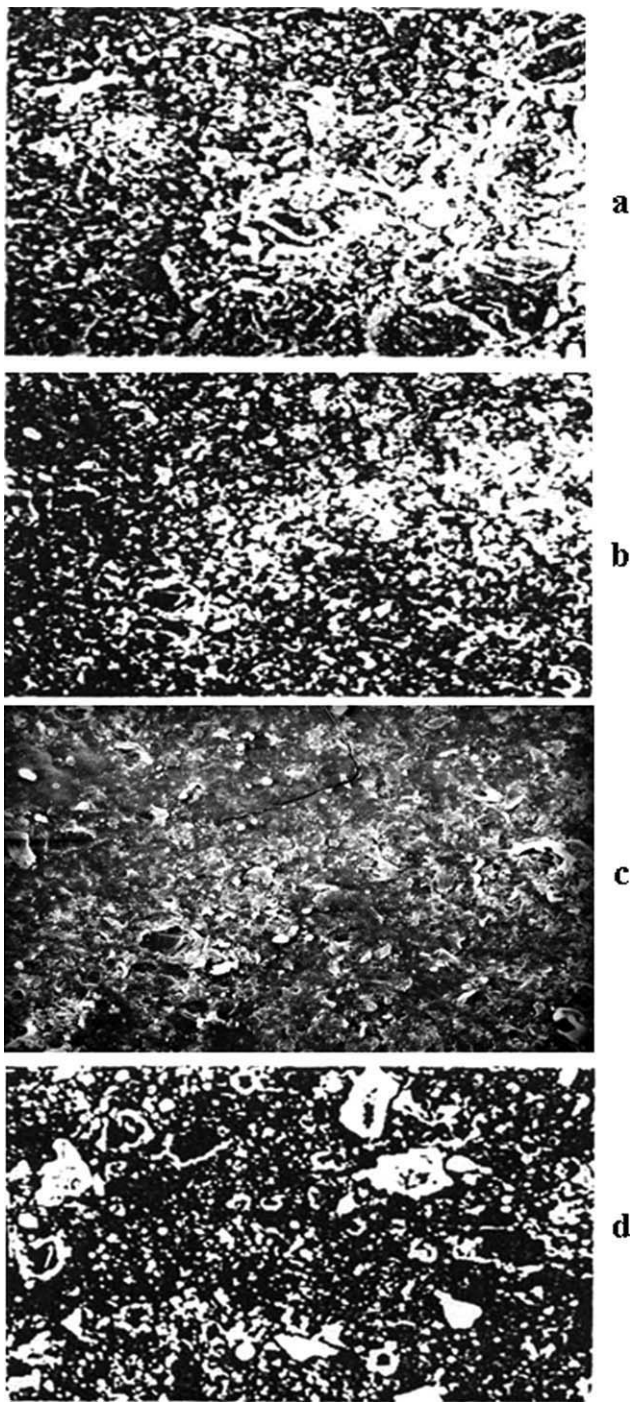

Figure 7 SEM micrographs of the SBR/graphite composites with different graphite contents (500×): (a) 10, (b) 30, (c) 50, and (d) 70 phr.

solvent, and χ is the interaction parameter between the rubber and toluene ($\sim$ 0.446 for SBR).

The variation of ν as a function of the graphite loading is given in Table IV. As shown in this table, increased with increasing graphite content and it was also high with smaller particle size; this indicated rubber-filler interaction.

Dielectric properties

The ε' and ε'' values of SBR filled with different concentrations and particle sizes of graphite were measured at room temperature ($\sim$ 30°C). The data obtained are illustrated graphically in Figure 6 at 100 Hz. As shown in Figure 6, clearly, the values of ε' and ε'' increased with increasing graphite content. This increase in the complex ε' is a typical response in any heterogeneous system where the conductivity and relative ε' of the constituent phases differ and is a result of an interfacial polarization phenomenon that occurs at the interfaces of dissimilar materials at low frequency. Moreover, it is interesting to observe that for samples containing up to 70 phr graphite, ε' was inversely proportional to the particle size; that is, ε' increased with decreasing graphite particle size.

Surface morphology studies

The surface morphology of the SBR/graphite composites was studied with SEM. The obtained SEM photomicrographs for 10, 30, 50, and 70 phr graphite-filled SBR composites are shown in Figure 7(a–d), respectively. The photographs show the homogeneity and good dispersion of the graphite filler throughout the samples. The observed change in the morphology of micrographs depended on the amount of graphite present. The domain size of the filler increased with increasing filler content; this may have been due to an increase in the filler–filler interaction or agglomeration of graphite filler [Fig. 7(c,d)]. It was clear from the morphology study that the particle size of graphite had no observable effect. This may have been due to the overlapping between the values of the particle sizes used.

CONCLUSIONS

In this study, graphite powder fillers with different concentrations and sizes were mixed with SBR rubber. It was found that

1. The rheometric characteristics showed that M_H increased with increasing graphite concentration and decreasing particle size. This indicated that there was an improvement in the filler–rubber interaction. This was also supported by SEM photographs, the increase in α_f and the decrease in swelling
2. The mechanical properties registered an increase with increasing graphite concentration and decreasing particle size. This indicated that graphite had a reinforcing effect in the SBR matrix.
3. ε' and ε'' increased sharply with increasing graphite content. Also, ε' was inversely proportional to the particle size.

The authors thank A. M. Ghoneim (Microwave Physics and Dielectrics Department, National Research Center, Dokki, Cairo, Egypt) for his continuous support.

References

1. Byers, J. T. In Rubber Technology, 3rd ed.; Mark, J. E.; Erman, B.; Eirich, F. R., Eds.; Elsevier: San Diego, 2005; Chapter 3, p 51.
2. Gilomini, P.; Brechet, Y. Mater Sci Eng 1999, 7, 8054.
3. Frohlich, J.; Niedermeier, W.; Luginsl, H. D. Compos A 2005, 36, 449.
4. Coran, A. Y. In Science and Technology of Rubber, 3rd ed.; Mark, J. E.; Erman, B.; Eirich, F. R., Eds.; Academic: San Diego, 2005; Chapter 8, p 339.
5. Renukappa, R. D.; Sudhaker, S. J Reinforced Plast Compos 2006, 25, 1173.
6. Hamed, G. R. Rubber Chem Technol 2000, 73, 524.
7. Zhang, L. Q.; Jia, D. M. Symp Int Rubber Conf A 2004, A, 46.
8. Yang, J.; Tian, M.; Jia, Q.-X.; Zhang, L.-Q.; Li, X.-L. J Appl Polym Sci 2006, 102, 4007.
9. Wu, Y.-P.; Zhao, Q.-S.; Zhao, S.-H.; Zhang, L.-Q. J Appl Polym Sci 2008, 108, 112.
10. Wang, M. Rubber Chem Technol 1998, 71, 520.
11. El-Nashar, D. E.; Ward, A. A.; Abd-El-Messieh, S. L. Kautsch Gummi Kunstst 2009, 62, 434.
12. Donnet, J.-B.; Bansal, R. C.; Wang, M.-J. Carbon Black: Science and Technology, 2nd ed.; CRC: Boca Raton, FL, 1993.
13. Valent, J. L.; Mora-Barrantes, I.; Carretero-Gonz, J.; Lopez-Manchado, M. A.; Sotta, P.; Long, D. R.; Saalwchter, K. Macromolecules 2010, 43, 334.
14. Heinrich, G.; Kluppel, M. Adv Polym Sci 2002, 160, 1.
15. Koga, T.; Hashimoto, T.; Takenaka, M.; Aizawa, K.; Amino, N.; Nakamura, M.; Yamaguchi, D.; Koizumi, S. Macromolecules 2008, 41, 453.
16. Schroder, A.; Kluppel, M.; Schuster, R. H.; Heidberg, J. Carbon 2002, 40, 207.
17. Bishai, A. M.; Ward, A. A.; Ghoneim, A. M.; Younan, A. F. Int J Polym Mater 2003, 52, 31.
18. Rattanasom, N.; Saowapark, T.; Deeprasertkul, C. Polym Test 2007, 26, 369.
19. Han, J. J.; He, X. L.; Guo, W. H.; Wu, C. F. Plast Rubber Compos 2007, 36, 154.
20. Das, A.; Ghosh, A. K.; Basu, D. K. Kautsch Gummi Kunstst 2005, 58, 230.
21. Ward, A. A. Ph.D. Thesis, Cairo University, 2003.
22. Jingjie, H.; Xiliang, Z.; Weihong, G.; Chifei, W. J Appl Polym Sci 2006, 100, 3707.
23. Ward, A. A.; Khalf, A. I. Kautsch Gummi Kunstst 2007, 60, 623.
24. Reffaee, A. S. A.; El Nashar, D. E.; Abd-El-Messieh, S. L.; Abd-El Nour, K. N. Polym Plast Technol Eng 2007, 46, 591.
25. Haghighat, M.; Zadhoush, A.; Nouri Khorasani, S. J Appl Polym Sci 2005, 96, 2203.
26. Ismail, M. N.; Ghoneim, A. M. Polym Plast Technol Eng 1999, 38, 71.
27. Hui, R.; Yixin, Q.; Suhe, Z. S. Chin J Chem Eng 2006, 14, 93.
28. Chung, D. D. L. J Mater Sci 2002, 37, 1475.
29. Tang, K. M.; Huang, K. J.; Li, C. Q. Rubber Ind 1995, 42, 723.
30. Mathew, G.; Huh, M. Y.; Rhee, J. M.; Lee, M. H.; Nah, C. J. Polym Adv Technol 2004, 15, 400.
31. Brinke, J. W. T.; Debnath, S. C.; Reuve-Kamp, L. A. E.; Noordermeer, J. W. M. Compos Sci Technol 2003, 8, 63.
32. Mandal, S. K.; Basu, D. K. Rubber Chem Technol 1994, 67, 672.
33. Flory, P. J.; Rehner, J. J Chem Phys 1943, 11, 512.